ARTICLE
Journal of Cellular Biochemistry 118:464–477 (2017)

Journal of Cellular Biochemistry

Reversal of the Migratory and Invasive Phenotype of Ras-Transfected Mammary Cells by Photodynamic Therapy Treatment

Gustavo Calvo,[1] Daniel Sáenz,[1] Marina Simian,[2] Rocío Sampayo,[3] Leandro Mamone,[1] Pablo Vallecorsa,[1] Alcira Batlle,[1] Adriana Casas,[1] and Gabriela Di Venosa[1]*

[1]*Centro de Investigaciones sobre Porfirinas y Porfirias (CIPYP), Hospital de Clínicas José de San Martín, CONICET, University of Buenos Aires, Av. Córdoba 2351 1er subsuelo, Ciudad Autónoma de Buenos Aires, Argentina*

[2]*Instituto de Nanosistemas & CEDESI, Universidad Nacional de San Martín. 25 de Mayo y Francia, San Martín, Provincia de Buenos Aires, Argentina*

[3]*Instituto de Oncología "Ángel H. Roffo", Av. San Martín 5481, Ciudad Autónoma de Buenos Aires, Argentina*

ABSTRACT

Photodynamic therapy (PDT) is a non-thermal technique for inducing tumor damage following administration of a light-activated photosensitizing drug (PS). In a previous work we found that PDT induces cytoskeleton changes in HB4a-Ras cells (human mammary breast carcinoma HB4a cells transfected with the *RAS* oncogene). In the present work we have studied the migratory and invasive features and the expression of proteins related to these processes on HB4a-Ras cells after three successive cycles of PDT using different PSs: 5-aminolevulinic acid (ALA), Verteporfin (Verte), *m*-tetrahydroxyphenylchlorin (*m*-THPC), and Merocyanine 540 (MC). A slight (1.25- to 2-fold) degree of resistance was acquired in cell populations subjected to the three successive PDT treatments. However, complete cell killing was achieved after a light dose increase. Regardless of the PS employed, all the PDT-treated populations had shorter stress fibres than the untreated control HB4a-Ras cells, and the number of dorsal stress fibres was decreased in the PDT-treated populations. E-Cadherin distribution, which was already aberrant in HB4a-Ras cells, became even more diffuse in the PDT-treated populations, though its expression was increased in some of them. The strong migratory and invasive ability of HB4a-Ras cells in vitro was impaired in all the PDT-treated populations, with a behavior that was similar to the parental non-tumoral HB4a cells. MMP-2 and -9 metalloproteinase activities were also impaired in the PDT-treated populations. The evidence presented herein suggests that the cells surviving PDT would be less metastatic than the initial population. These findings encourage the use of PDT in combination with other treatments such as intraoperative or post-surgery therapeutic procedures. J. Cell. Biochem. 118: 464–477, 2017.

KEY WORDS: PHOTODYNAMIC THERAPY; PDT; *RAS* ONCOGENE; INVASION; MIGRATION; METASTASIS

Photodynamic therapy (PDT) is a non-thermal technique for inducing tissue damage with light following administration of a light-activated photosensitizing drug, which can be selectively retained in malignant or diseased lesions and not in normal adjacent tissues [Dougherty, 2002]. Under the catalyzing effect of light, the photosensitizer (PS) reacts with oxygen molecules to form cytotoxic oxygen species. PDT requires the simultaneous use of light and a PS; therefore, the development of different levels of cell resistance will depend on the doses of PS and/or the light dosage used during treatment [Casas et al., 2006]. PDT is a therapeutic strategy to be applied, either alone or in combination with other treatments for both oncological and non-oncological pathologies. In addition to its use in dermatology, PDT has proved to have a great potential for palliative and even curative treatment of endoscopically accessible

Abbreviations: ALA, 5-aminolevulinic acid; ECM, extracellular matrix; LD_{50}, light dose 50; MC, merocyanine 540; MI, migratory index; m-THPC, *m*-tetrahydroxyphenylchlorin; MTT, 3-[4,5-dimethylthiazol-2-yl]-2,5-diphenyltetrazoliumbromide; PpIX, protoporphyrin IX; PDT, photodynamic therapy; *p*-FAK, phosphorylated focal adhesion kinase; PS, photosensitizer; Verte, Verteporfin.

Grant sponsor: CONICET; Grant sponsor: Science and Technology Argentine Agency; Grant numbers: PICT 2010-0772, PICT 2008-0047.

*Correspondence to: Dr. Gabriela Di Venosa, Centro de Investigaciones sobre Porfirinas y Porfirias (CIPYP), Hospital de Clínicas José de San Martín, CONICET, University of Buenos Aires, Av. Córdoba 2351 1er subsuelo, Ciudad Autónoma de Buenos Aires, Viamonte 1881 10A, 1056 Buenos Aires, Argentina. E-mail: gabrieladivenosa@yahoo.com.ar

Manuscript Received: 20 April 2016; Manuscript Accepted: 19 July 2016

Accepted manuscript online in Wiley Online Library (wileyonlinelibrary.com): 20 July 2016

DOI 10.1002/jcb.25657 • © 2016 Wiley Periodicals, Inc.

tumors, such as lung and bladder carcinomas and it is increasingly being used for the treatment of gastrointestinal and gynecological neoplasms as well as head and neck cancer [Dolmans et al., 2003]. The major advantage of the use of PDT is the possibility to perform a local treatment, thus preventing systemic side effects of conventional therapies. The aim of the intraoperative application of PDT to target primary tumor satellites occurring in the surrounding tissues after surgical tumor resection is to decrease the number of recurrences and to reduce the risk of occurrence of post-operative metastases [Meier et al., 2014].

There are several natural and synthetic compounds with photosensitizing properties, and it is believed that the subcellular location and its response to PDT strongly depend on the nature of the PS. One of the most useful and effective PS, is Protoporphyrin IX (PpIX), which is endogenously synthesized after the administration of 5-aminolevulinic acid (ALA) [Kelty et al., 2002]. The main clinical application of ALA-PDT has been the topical treatment of non-melatomatous skin lesions, mainly for basal cell carcinoma; although the Food and Drug Administration approval has only been granted for the treatment of actinic keratosis [Tanghetti et al., 2015] and Bowen disease [Cai et al., 2015]. Other approved PSs include porphyrins such as Verteporfin (Verte), which is a Benzoporphyrin derivative, for the treatment of wet age-related macular degeneration, and chlorins such as *m*-tetrahydroxyphenylchlorin (*m*-THPC). Foscan is the trademark for *m*-THPC that has successfully been used for the treatment of head and neck cancer. Merocyanine 540 (MC) is a dye that has been employed for the treatment of infections and haematological tumors [Sieber et al., 1987].

The effectiveness of the photodamage induced by PSs in both cell cultures and tumors is related to their chemical structure, concentration, incubation time, vehicle, light dose, and site of sub-cellular localization. Numerous cell components have been described to be targets for the cytotoxic effects of PDT, including mitochondria, lysosomes, Golgi apparatus, plasma membrane, and nucleus. PSs localising in mitochondria and lysosomes are highly effective, triggering either apoptosis or necrosis [Stockert et al., 2004].

While porphyrins such as PpIX and Verte are mainly accumulated in mitochondria [Runnels et al., 1999], *m*-THPC has been suggested to accumulate in lysosomes [Leung et al., 2002]. On the other hand, MC enters the cell but it accumulates at the plasma membrane, thus the membrane lipids are considered to be the targets of photodamage [Diwu and Lown, 1994].

Three major eukaryotic cytoskeletal proteins are actin, tubulin and intermediate filaments, and disturbances in these systems have been related to tumor progression and the development of metastasis [Lambrechts et al., 2004]. Cell adhesion to substrata is mediated by integrins and other cell adhesion molecules which link the extracellular matrix (ECM) to the intracellular actin cytoskeleton. Vinculin is a multi-ligand cytoskeleton protein that is known to link actin filaments with integrins. Vinculin is localized in focal contacts and its reduced expression has been correlated with increased metastasis development [Li et al., 2014].

Focal adhesion kinase (FAK) is a prominent component of the cellular substratum attachment point. This kinase undergoes rapid phosphorylation on tyrosine residue 397 in response to adhesion and numerous extracellular stimuli. FAK is critically positioned to integrate signals from the ECM and cellular adhesion. It is essential for normal vascular development and has been demonstrated to participate in a wide range of cellular functions, including the regulation of cell proliferation, migration, differentiation, and survival. Particularly, the phosphorylated form of FAK (*p*-FAK) has been associated to invasiveness in certain cancers [Sulzmaier et al., 2014].

Alterations in any of the three major components of cytoskeleton have been related to tumor progression and metastasis development. The loss of E-cadherin expression leads to epithelial tumorigenesis. Deregulation of E-cadherin adhesion is a crucial step during cell migration and metastasis and, therefore, many epithelial cancer cells can dynamically downregulate E-cadherin expression to initiate the migration process [Hazan et al., 2004].

Actin plays a role in biological processes such as sensing environmental forces, internalizing membrane vesicles, moving over surfaces, and mitosis. The abnormal expression and polymerization of actin and the resulting changes in the cytoskeleton are associated with the invasiveness and metastasis of cancers [Guo et al., 2013]. It is well known that cancer cell migration often involves cell-to-cell and cell-to-substrate adhesions and a highly coordinated motion of adjacent cells.

Cytoskeletal structures are also clearly affected by photosensitization. Increasing evidences suggest that PDT also induces cell-membrane damage and alterations in cancer cell adhesiveness [Di Venosa et al., 2015]. Actin has been identified as a cytoskeleton component mainly affected by PDT either at early or at late stages of photodamage, although dynamic alterations on E-cadherin and integrins expression after photodynamic treatment have also been reported [Di Venosa et al., 2015].

Stress fibres are composed of bundles of approximately 10–30 actin filaments. These bundles are held together by the actin-crosslinking protein α-actin. In motile cells, the majority of stress fibres show overall graded polarity—at each end of the fibre the filament polarity is uniform, barbed ends pointing outwards, but the distribution of filament polarities becomes mixed at the centre of the fibre. The stress fibres observed in fibroblasts have been divided into three classes on the basis of their subcellular location: ventral stress fibres, dorsal stress fibres, and transverse arcs. Ventral stress fibres are the most commonly observed structures and lie along the base of the cell, attached to integrin-rich focal adhesions at each end. Dorsal stress fibres are attached to a focal adhesion at one end only, which tethers them to the base of the cell [Pellegrin and Mellor, 2007].

Ras proteins play a direct causal role in human cancer and in other diseases. Mutant H-, N-, and K-Ras occur in 20–30% of all human tumors [Rodriguez-Viciana et al., 2005]. Proteins of the Ras family are very important molecular switches for a wide variety of signal pathways that control processes such as cytoskeletal integrity, proliferation, cell adhesion, apoptosis, and cell migration. The expression of Ras and Ras-related proteins is often deregulated in cancers, leading to increased invasion and metastasis, and a decreased apoptosis rate [Rodriguez-Viciana et al., 2005].

In a previous work, we found that the insertion of Ras induced per se a distribution disorganization of both F-actin and E-cadherin on

the normal human immortalized mammary HB4a cells. When the normal HB4a cells are treated with ALA-PDT, a transient disorganization of actin stress fibres was also observed, resembling the non-treated Ras-transfected cells. It is noteworthy that even 48 h after treatment, some features of F-actin disorganization remain in HB4a surviving cells, resembling the Ras-transfected ones, thus suggesting that some degree of microfilament damage persists after photodamage. On the other hand, PDT did not impact on E-cadherin distribution; only a transient disorganization was observed, which was reverted after 24 h [Di Venosa et al., 2012].

Considering that PDT induces morphological changes as well as actin reorganization in HB4a-Ras cells, in the present work we studied the impact of successive cycles of PDT on its migratory and invasive features and the expression of the related proteins employing different PSs acting at different subcellular levels. This information could be useful to optimize the use of PDT as an anticancer treatment.

MATERIALS AND METHODS

CHEMICALS

ALA, MC, and MTT were obtained from Sigma Chem. Co. Verteporfin was obtained from Conifarma, Argentina, and *m*-THPC (Foscan®) was purchased from Biolitec Pharma Ltd., Ireland.

The anti-mouse monoclonal antibody against E-cadherin was obtained from Transduction Laboratories, UK and the anti-mouse IgG secondary antibody conjugated to Alexa Fluor 488 was purchased from Molecular Probes, Oregon. For F-actin detection, phalloidin-labeled with tetramethylrhodamine isothiocyanate (TRITC, Sigma, UK) was employed.

The anti-mouse monoclonal antibodies against β1-integrin and *p*-FAK were obtained from Transduction Laboratories, UK; the antibody against β-actin was purchased from GE Healthcare UK Ltd., Buckinghamshire, UK, and the antibody against vinculin was bought from Sigma. For Western blot analysis, the secondary antibodies employed were peroxidase-conjugated goat anti-mouse IgG (Jackson ImmunoResearch Laboratories, Inc., West Grove, PA) and peroxidase-conjugated donkey anti-rabbit IgG (GE Healthcare).

CELL LINES

The HB4a is a clonal, non-transformed, non-tumorigenic cell line derived from reduction mammoplasty tissue. It is one of a panel of immortal cell lines developed by means of an amphotropic retrovirus to transduce the SV40-derived recombinant viral oncogene mutant ts*A58-U19* into luminal epithelial cells which had been sorted by FACS using the lumen-specific marker epithelial membrane antigen [Stamps et al., 1994]. HB4a r4.2 (HB4a-Ras) cells were generated by transfecting HB4a parental cells with the pEJ plasmid containing a 6.6-Kb genomic H-Ras (VAL/12 Ras) sequence [Rusnak et al., 2001]. Both cell lines were a gift from Prof. Michael O'Hare from the Department of Surgery, University College London. Cells were maintained at 37°C (5% CO_2) in RPMI 1640 medium with L-glutamine, supplemented with 10% foetal bovine serum (FBS), 5 μg/ml hydrocortisone and 5 μg/ml insulin.

PDT-TREATED CELL POPULATIONS

HB4a-Ras cells were treated with Verte (3 h, 2 μg/ml, 130 mJ/cm^2), MC (2 h, 3 μg/ml, 30 mJ/cm^2), *m*-THPC (3 h, 1 μg/ml, 20 mJ/cm^2), or ALA (3h, 1 mM, 130 mJ/cm^2), which are conditions known to induce around 95% of cell death. Cells were maintained until confluency and an aliquot of the initial cell population, named PS1, was frozen while surviving cells (~5%) were allowed to recover to be treated again to obtain a second population (PS2); the same procedure was carried out with PS2 and the third population was obtained (PS3). Light doses but not PS doses were increased to obtain 95% of cell death in the second and third PDT cycles. Both PS2 and PS3 populations were frozen and kept under a nitrogen atmosphere until used. Since the recovery time was different for each PDT cycle and PS employed, PDT sessions were performed at different times for each cell population and each PS.

In all, 12 cell populations were obtained and named as follows: ALA1, ALA2, ALA3, Verte1, Verte2, Verte3, MC1, MC2, MC3, *m*-THPC1, *m*-THPC2, and *m*-THPC3.

The established PS1, PS2, and PS3 populations proved to be stable in terms of resistance at least for 10 months after the last treatment and all the experiments were carried out within that time period. After thawing the cell populations were allowed two cell cycles to recover before performing the experiments. Each experiment was carried out simultaneously employing the 12 populations obtained.

MTT VIABILITY ASSAY

Phototoxicity and cell viability were assessed by the MTT assay [Denizot and Lang, 1986], which is a method based on the activity of mitochondrial dehydrogenases. Following appropriate treatments, a MTT (3-[4,5-dimethylthiazol-2-yl]-2,5-diphenyltetrazoliumbromide) solution was added to each well in a concentration of 0.5 mg/ml, and plates were incubated at 37°C for 1 h. The resulting formazan crystals were dissolved in dimethyl sulfoxide and the absorbance was read at 560 nm.

CELL GROWTH AND CELL DOUBLING TIME

1×10^5cells/ml were seeded in triplicate in 24-well plates. Every 2, 24, 48, and 72 h, cells were counted in a haemocytometer. The doubling time was estimated at the midpoint of the exponential phase of the growth curve.

PDT TREATMENT

Cells (1×10^5 cells/ml) were incubated in serum-free medium containing the PSs in the time and concentrations conditions indicated in Table I, which allowed a significant photosensitization employing the desired light dose range. Immediately afterwards, the illuminations were performed employing the light source system described below. After illumination, the medium was replaced by PS-free medium + serum, and cells were incubated for another 19 h and evaluated for viability by the MTT assay. Lethal light doses 50 (LD_{50}) were defined as the light doses expressed in mJ/cm^2, necessary to kill 50% of cells.

LIGHT SOURCE

A bank of two fluorescent lamps (Osram L 18W/765) was used. The light spectrum was between 400 and 700 nm with the highest radiant power at 600 nm. Plates were located at a distance of 14 cm from the

TABLE I. Conditions of PDT Treatments and PSs Extraction From Cells

	PpIX (ALA)	Verte	MC	m-THPC
Incubation time (h)	3	3	2	3
Concentration	1 mM	2 μg/ml	3 μg/ml	1 μg/ml
Extraction solvent	5% HCl	MeOH: H_2O (1:1)	EtOH: AcOH: H_2O (70:5:25)	MeOH: DMSO (4:1)
Excitation λ (nm)	406	420	520	423
Emission λ (nm)	604	690	580	657
References	Casas et al. [2001]	Casas et al. [2002]	Rundquist et al. [1984]	Cai et al. [1999]

light source, and the cells were irradiated from below. The fluence rate was measured with a FieldMaster power-meter and a LM3 HTP sensor (Coherent Inc.). We used fluences between 5 and 150 mJ/cm^2 and power density was 0.5 mW/cm^2.

PS EXTRACTION FROM CELLS

Cells (1×10^5 cells/ml) were plated in 24-well plates and employed after 48 h under semi-confluency conditions. Cells were incubated in the presence of the PSs in serum-free medium under conditions previously determined and depicted in Table I. Afterwards, intracellularly accumulated PSs were extracted and quantified fluorometrically employing a Perkin–Elmer LS 55 LuminescenceSpectrometer. PpIX, Verte, MC and *m*-THPC were dissolved in the corresponding solvents (Table I) and were used as reference standards. The extraction solvents employed for each PS are detailed in Table I.

CELL PROTEIN DETERMINATION

Cells (1×10^5 cells/ml) were plated in 6-well plates and employed 24 h later. After three washings with PBS, cells were kept overnight in the presence of 1 N NaOH. Protein content was then determined by the Lowry method. Bovine seroalbumin (BSA) was used as standard.

IN VITRO MIGRATION ASSAY

Cell migration of cells surviving PDT, that is PS1, PS2, and PS3 was determined using a wound healing assay. An amount of 2×10^5 HB4a and HB4a-Ras cells and each population (PS1, PS2, and PS3) were plated in complete medium containing 10% FBS into six-multiwell plates and allowed to grow until confluency, time at which the cultures were wounded. Cells were then gently wounded through the central axis with a sterile 200 μl tip. Cells were washed with PBS and refreshed with medium with serum. After overnight incubation (21 h) at 37°C, cells were fixed, stained with Crystal violet and photographed. Quantification of cell motility was performed by measuring the distance between the invading front of cells in six random selected microscopic fields for each condition. The degree of motility was expressed as a migration index $\left(\mathrm{MI} = \frac{0\text{ h wound} - 24\text{ h wound}}{0\text{ h wound}}\right)$. Images were acquired with an Olympus microscope with 4X objective and processed using image processing software.

IMMUNOFLUORESCENCE ASSAY

For general immunodetection, cells (1×10^5 cells/ml) grown on coverslips were fixed in 4% paraformaldehyde for 15 min. Samples were rehydrated in PBS, permeabilized with 1% Triton X-100 in PBS for 10 min and incubated with the anti E-cadherin primary antibody for 1 h at 37°C, washed with PBS, incubated with a FITC-labeled secondary antibody (1:500 in 0.1% BSA) and finally washed with PBS. For F-actin detection, cells were incubated with TRITC-phalloidin (1:500 of a 1 mg/ml initial solution in 0.1% BSA) for 15 min at 37°C and washed with PBS. The preparations were mounted in ProLong Gold antifade reagent (Invitrogen). Microscopic observation and photography were performed with an Olympus photomicroscope BX51, equipped with a HBO 100 W mercury lamp and the corresponding filter sets for fluorescence microscopy: blue (450–490 nm, exciting filter BP 490) and green (545 nm, exciting filter BP 545).

CELL ADHESION ASSAY

Cell adhesion was determined in HB4a, HB4a-Ras, and in the 12 populations obtained after the successive treatments. Twenty-four well plates were employed. Cells (1×10^5 cells/ml) were trypsinized and plated in medium with serum. After 30 min incubation at 37°C, cells were washed three times with PBS. The remaining adherent cells were fixed in methanol: acetone (1:1) for 15 min and stained with 0.5% Crystal violet. Adherent cells were quantified by measuring the absorbance at 560 nm after solubilization in 2% sodium dodecyl sulfate. Adhesion values were determined in quadruplicate.

INVASION TRANSWELL ASSAYS

Cell invasion was determined in HB4a, HB4a-Ras, and in the 12 populations obtained after the successive treatments. Transwell Permeable Supports (Corning Incorporated, NY) were coated with diluted Matrigel. Exponentially growing cells (4.5×10^5 cells/filter) suspended in medium without serum, were added to the upper chamber. The lower chamber, which had been prefilled 10% serum containing medium as chemoattractant, was then assembled. After 20 h incubation at 37°C, the cells on the upper surface of the filter were removed with a cotton swab. Time and cell density conditions had been previously determined. Filters were fixed with ice-cold methanol and stained with 0.1% Crystal violet. The degree of invasion was measured by counting the number of cells in the lower surface of the filter at 400× magnification.

DETECTION OF METALLOPROTEASES (MMP) ACTIVITY

Cells (1×10^5 cells/ml) were plated in 6-well plates and employed 24 h later. The collagenolytic activity secreted by the cell populations was determined in conditioned media by gel electrophoresis using SDS and polyacrylamide copolymerized with 0.1% gelatin. The protein content in the cells was determined by the Lowry method. The conditioned media were adjusted to the same protein concentration. To detect specific activity after running, gels were washed in 2% Triton X-100 and incubated for 72 h in a buffer containing 0.25 M Tris–HCl, 1 M NaCl and 25 mM $CaCl_2$ (pH 7.4). To detect non-specific activity, 40 mM EDTA was added to the buffer solution. Gels were fixed and stained with Coomassie Blue. Gelatinolytic bands were identified by negative staining and quantified by an image densitometer coupled to an image analyser. MMP-2 and -9 activities of PDT-treated populations were expressed as a percentage of the HB4a-Ras cells.

WESTERN BLOT ASSAYS

Cells (1×10^5 cells/ml) were plated in 6-well plates and employed 24 h later. The monolayers were washed and then lysed with RIPA buffer [150 mM NaCl, 1% Triton X-100, 0.05% deoxycholate, 0.1% SDS, 1% Nonidet-P40, 50 mM Tris (pH 8)] containing Phosphatase cocktail 2 and Protease inhibitor cocktail (Sigma). Samples were adjusted to the same protein concentration (Bicinchoninic acid, BCA protein assay kit, Pierce, Rockford, IL), denatured by boiling in Laemmli sample buffer containing 5% β-mercaptoethanol and resolved by SDS–PAGE. Gels were electroblotted to a PDVF Immobilon-P membrane (Millipore, Bedford, MA), blocked with 5% skim milk in Tris-buffered saline (10 mM Tris–HCl pH 7.6, 0.9% NaCl, 0.05% Tween 20) overnight at 4°C. Afterwards, membranes were incubated 1 h at room temperature with primary specific antibodies diluted in blocking buffer. The secondary antibody was used at a 1:10,000 dilution and incubated 1 h at room temperature. Detection was performed using the ECL Plus Western blotting detection system (GE Healthcare UK limited, Buckinghamshire, UK). Bands were quantified by scanning on a digital GS-700 densitometer employing the Molecular Analyst software and analysed for comparison.

STATISTICAL ANALYSIS

Values in figures and tables were expressed as mean ± standard deviations of the means. A two-tailed Student's *t*-test was used to determine statistical significance between means.

RESULTS

CHARACTERIZATION OF PDT-TREATED CELL POPULATIONS

Both HB4a-Ras cells and the PDT-treated populations showed similar characteristics in terms of protein content (28.9 ± 5.2 pg/cell), doubling time (32 ± 2 h) and MTT activity.

ADHESION TO PLASTIC

Even when the cell doubling time was similar, we observed that in most of the PDT-treated populations, the amount of cells was increased 48 h after plating, as compared to the HB4a-Ras parental cells. These findings led us to hypothesize that the PDT-treated populations were more adherent to the plastic.

Figure 1 shows an adhesion assay to plastic. HB4a cells are per se significantly more adherent than their *RAS* transfected counterpart. The population of cells treated with ALA, MC, and *m*-THPC showed plastic adhesion properties that increased with the number of PDT cycles, whereas when Verte was employed as PS, adhesion decreased in the Verte3 population. Adhesion values were significantly higher than those corresponding to HB4a-Ras cells receiving two and three cycles of MC and *m*-THPC-PDT and three cycles of ALA-PDT. The most adherent population was the MC3, where adhesion values were 2.3-fold higher. The increased adhesion in PDT-treated cells was similar to the degree of adhesion of the non-transfected HB4a cells.

These different adhesion patterns were taken into account when plating the cells, so that an equal amount of cells were present at 48 h after seeding.

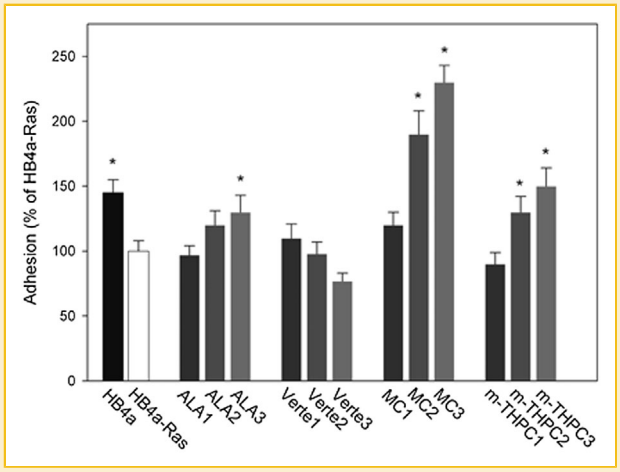

Fig. 1. Cell adhesion of HB4a, HB4a-Ras, and PDT-treated populations. After 30 min of culture on plastic (1×10^5 cells/ml), cell adhesion was determined using a colorimetric method described in Materials and Methods. Results are presented as means ± SD from four individual samples. $^*P < 0.05$ compared to HB4a-Ras (Student's *t*-test).

MICROFILAMENT PATTERN

In a previous work, we have demonstrated that in non- treated HB4a cells, large stress fibres are organized along the cytoplasm [Di Venosa et al., 2012]. Many HB4a-Ras cells have large stress fibres mainly organized at the cell periphery, some of them assembled in actin microspikes protruding from dorsal fibres, some of them organized in a cortical actin rim. As a rule, all PDT-surviving populations exhibited shorter stress fibres than the parental ones, with a decreased number of dorsal fibres (Fig. 2), independently of the PS employed. The circumferential cortical actin ring is conserved in the PDT-treated cells. Actin surface blebbing is observed in some of the populations. The latter is a feature that has been previously reported by us to be a photodamage-induced transient change [Di Venosa et al., 2012].

These changes on actin disorganization probably correlate with the different shape of the sub-populations. One of the salient features of the PDT-treated cells was the increasing loss of cell-to-cell interactions. Even though the insertion of Ras had already modified the epithelial features of HB4a cells, PDT-treated cells underwent a further loss of their epithelial morphology.

E-CADHERIN IMMUNOSTAINING

While HB4a cells exhibit a normal E-cadherin distribution at the cell-to-cell interface, such distribution is disrupted in *RAS*-transfected cells. E-cadherin expression is aberrant in HB4a-Ras cells, with numerous interdigitations appearing along the cell-to-cell interface, where a diffuse cytoplasmic signal of E-Cadherin is also present. In the surviving cell populations obtained after successive PDT treatments, no E-cadherin signal was found at the cell-to-cell interface, and the protein was found to be diffusely distributed through the whole cytoplasm in spot-shaped clusters. Representative photographs of the subpopulations PS3 are shown in Figure 3.

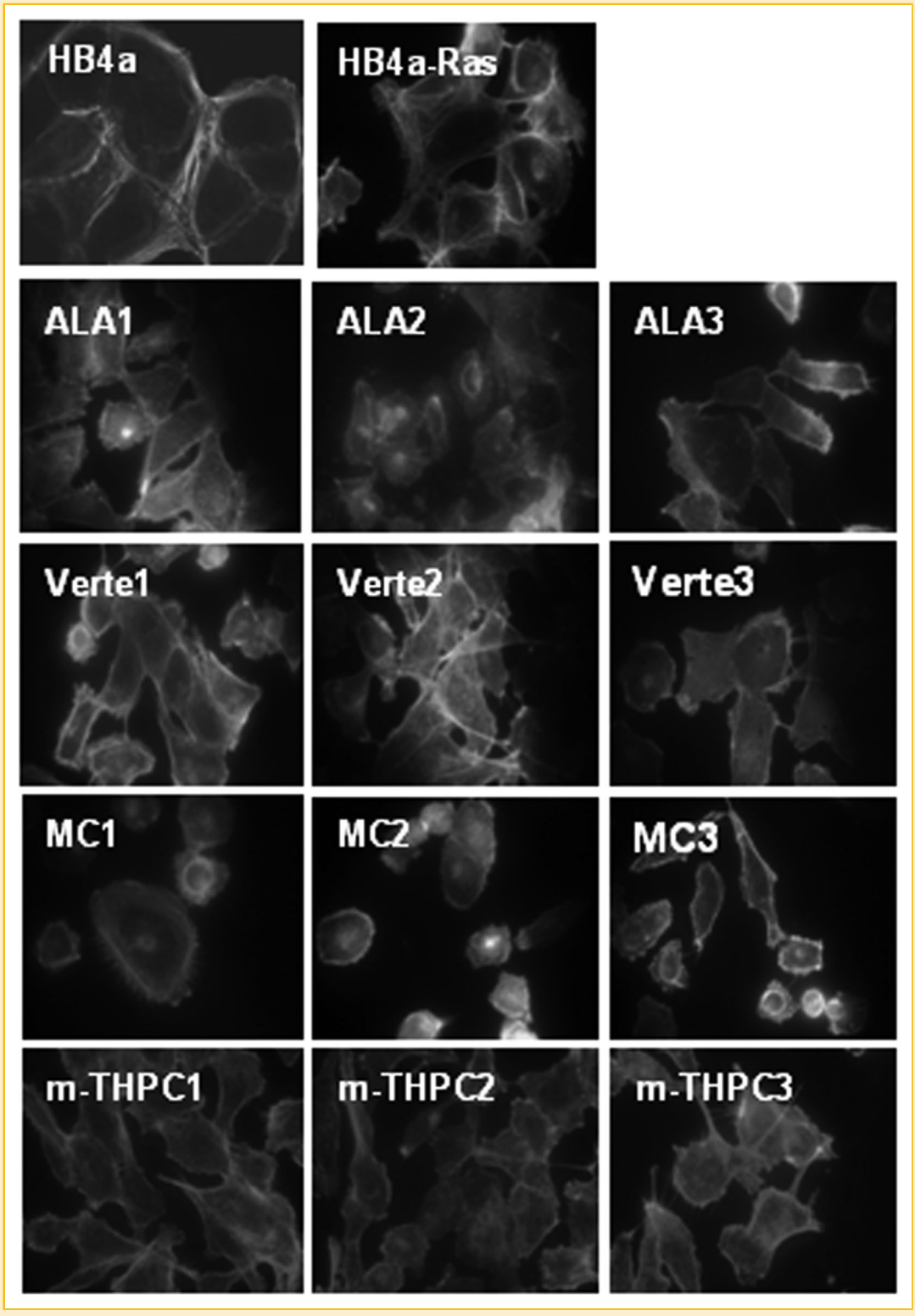

Fig. 2. Micrographs of microfilaments in HB4a, HB4a-Ras cells, and PDT-treated populations. Subconfluent monolayers were fixed and stained for F-actin using TRITC-phalloidin (F-actin) as described in Materials and Methods. Magnification 100×.

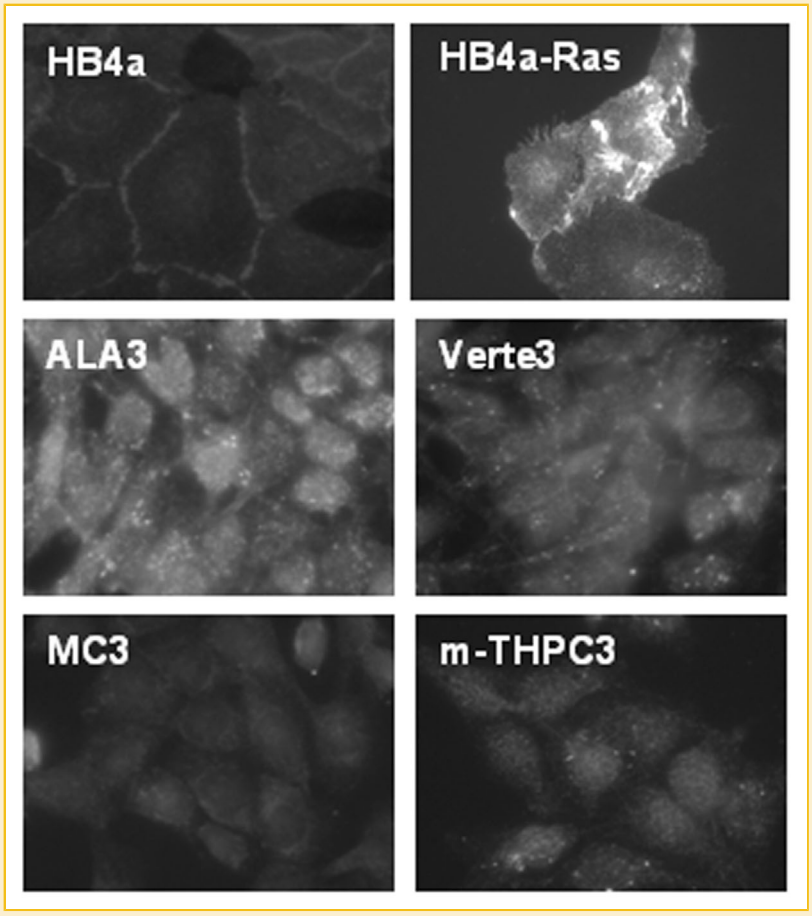

Fig. 3. Immunostaining for E-cadherin in HB4a, HB4a-Ras cells, and PDT-treated populations. Subconfluent monolayers were fixed and indirect immunodetection of E-cadherin was carried out employing a FITC-labeled secondary antibody as specified in Materials and Methods. Magnification 100×.

CELL MIGRATION ASSAY

The migratory capacity of the PDT-treated populations was studied in vitro in comparison with the initial HB4-Ras cells (Fig. 4). In these experiments, the parental HB4a cells non-transfected with the *RAS* oncogene were also included.

The strong migratory capacity of HB4a-Ras cells was found to be dramatically impaired in all the PDT-treated populations, thus resembling the parental HB4a normal cells. The migratory capacity was found to decrease with the number of PDT cycles for all the PSs employed.

Even one PDT cycle was capable of inducing a significant reduction in the cell migration rate. The most affected populations were ALA3, Verte3, MC3, and *m*-THPC3, which exhibited a 2-, 2.4-, 2.5-, and 3.1-fold migration reduction, respectively.

TRANSWELL INVASION ASSAY

Figure 5 depicts the invasion ability of the PDT-treated populations as compared to the HB4a-Ras cells and its parental HB4a non-transfected counterpart. The migration rate obtained with HB4a-Ras cells was considered 100% of migration while the invasion rate exhibited by HB4a cells was 0%.

From two PDT cycles onwards, all the subpopulations showed a significantly impaired invasion capacity, whereas ALA-PDT-treated cells displayed a significantly lower invasion capacity than the HBa-Ras cells, even after only one PDT session.

For all the PSs employed, the decreased invasion capacity correlated negatively with the number of PDT cycles. After three PDT cycles, the percentages of invasion ranged from 10 to 0.6%, depending on the PS employed, being MC3 the most effective on tampering the in vitro invasion. An almost total blockade of the process could be achieved, which meant reverting the Ras invasive phenotype.

METALLOPROTEASES ACTIVITY

The gelatinolytic activity of the PDT-treated subpopulations was quantified and compared to HB4a-Ras activity. MMP-9 and -2 activities were quantified in cell conditioned medium (Fig. 6). Except for ALA, for the rest of the PSs, a correlation between the number of PDT cycles and diminution of activity was observed for both metalloproteinases.

The most affected populations were the MC-PDT treated ones, which maintained only around 50% of the initial activity even after only one PDT cycle.

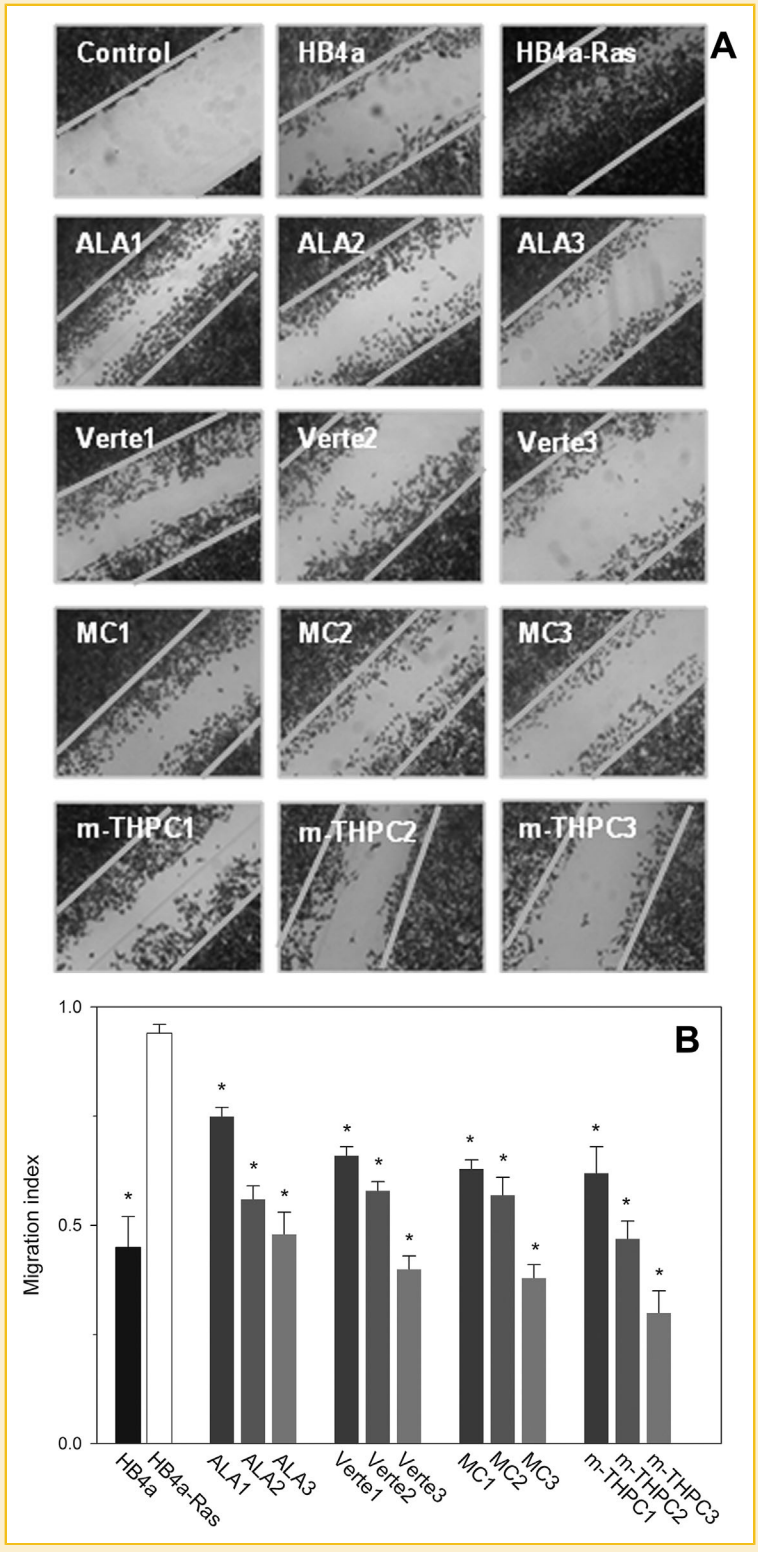

Fig. 4. In vitro migration assay of HB4a, HB4a-Ras, and PDT-treated populations. Images were taken at 21 h after the wound healing. Controls of time 0 were carried out immediately after wounding (A). Quantification of cell motility by measuring the distance between the invading fronts of cells in six random selected microscopic fields. The degree of motility is expressed as MI as detailed in Materials and Methods (B). $^{*}P < 0.05$ compared to HB4a-Ras (Student's *t*-test).

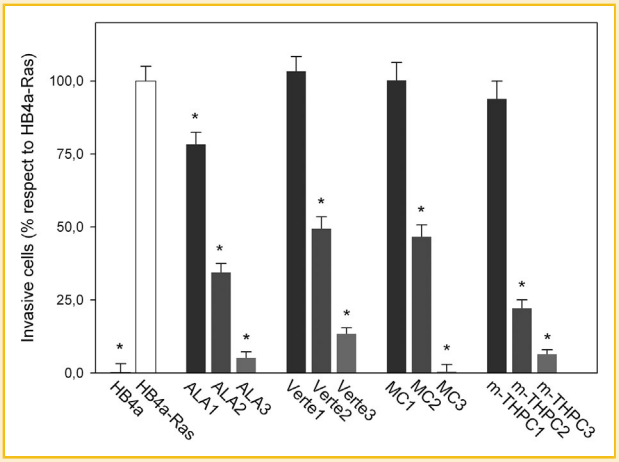

Fig. 5. In vitro invasion assay of HB4a, HB4a-Ras, and PDT-treated populations. Cell invasiveness was tested in vitro in Matrigel-coated inserts as was described in Materials and Methods. Bars represent means ± SD of four independent experiments run in triplicate. Results are expressed as percentage of total cells plated in the inserts. $^{*}P < 0.05$ compared to HB4a-Ras (Student's *t*-test).

WESTERN BLOT ASSAYS

The expression of several proteins involved in the processes of cell adhesion to substrata or cell-to-cell adhesion such as vinculin, β1-integrin, E-cadherin, and *p*-FAK was quantified in the PDT-treated populations and the HB4a-Ras cells (Fig. 7). None of the proteins were significantly and consistently altered in the PDT-treated populations as compared to HB4a-Ras. E-Cadherin was randomly increased in some of the PDT-treated populations; however, no correlation was found between the number of PDT cycles and an increased protein expression.

RESPONSE TO PHOTODYNAMIC THERAPY

The outcome of PDT was evaluated as a function of the light dose in HB4a-Ras cell line and its derived PDT-treated populations (Fig. 8). A slight degree of resistance was acquired upon the successive treatments. However, an increase of the light dose employed led to complete cell killing.

The LD_{50} for each PS increased as a function of the number of PDT cycles. LD_{50} was 60 mJ/cm^2 after ALA-PDT treatment whereas, for ALA3 population LD_{50} increased twofold to reach a value of 120 mJ/cm^2.

Similarly, LD_{50} changed from 60 to 90 mJ/cm^2 after three Verte-PDT cycles, which represents a 1.5-fold light dose increase.

Moreover, for MC-PDT treated populations, LD_{50} increased from 20 to 25 mJ/cm^2 (1.25-fold) and from 7 to 15 mJ/cm^2 for *m*-THPC (2.1-fold).

It is worth mentioning that under the above mentioned conditions, the synthesis of Protoporphyrin IX from ALA (29.1 ± 3.4 ng PpIX/10^5 cells) as well as the intracellular incorporation of Verte (242 ± 28 ng Verte/10^5 cells), MC (49 ± 5 ng MC/10^5 cells), and *m*-THPC (74 ± 6 ng *m*-THPC/10^5 cells) was not significantly different between HB4a-Ras cell line and its derived PDT-treated populations.

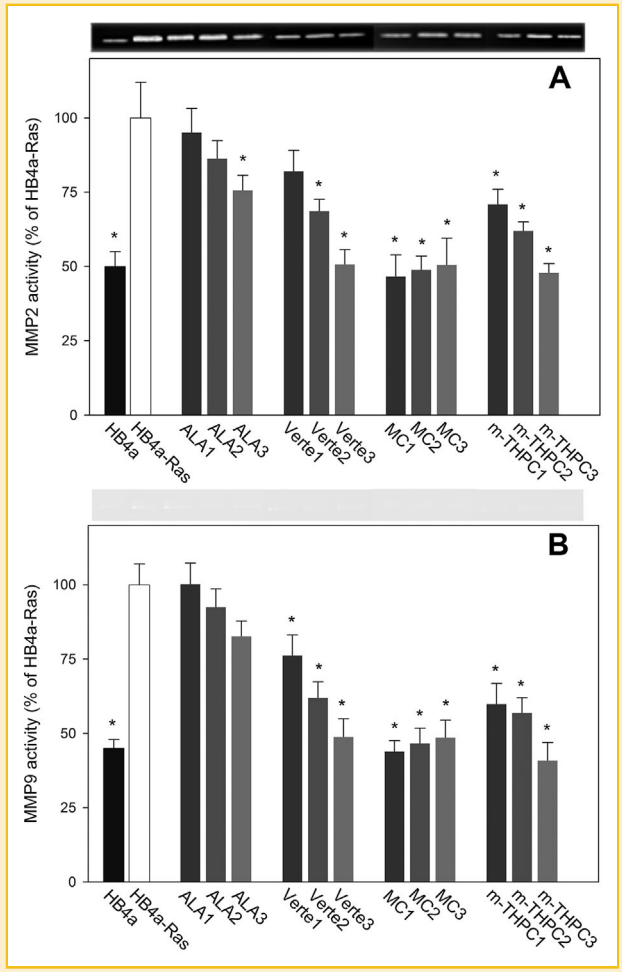

Fig. 6. Collagenolytic activity of conditioned culture media of HB4a, HB4a-Ras, and PDT treated populations MMP-2 (A) and -9 (B) activities were determined as described in Materials and Methods and were expressed as percentage of the HB4a-Ras cells. $^{*}P < 0.05$ compared to HB4a-Ras (Student's *t*-test). A representative image of a gelatinzymogram is shown.

DISCUSSION

In a previous work, we have demonstrated that the human mammary HB4a-Ras cell line exhibits intrinsic resistance to ALA-PDT, as compared to its normal HB4a counterpart; even when they produce a lower amount of the PS Protoporphyrin IX [Rodriguez et al., 2007]. Moreover, we have also described the changes in the actin pattern induced by ALA-PDT treatment on both HB4a and HB4a-Ras cells [Di Venosa et al., 2012].

We have also reported that ALA-PDT resistant clones derived form a murine adenocarcinoma exhibited not only changes on F-actin and E-cadherin distribution, but also a completely impaired capacity to invade and migrate both in vitro and in vivo [Casas et al., 2008a,b]. As expected, a certain degree of resistance (1.25- to 2-fold) was acquired, which was also proportional to the number of PDT sessions. However, all the cell populations remained sensitive to PDT when the light dose was increased.

In the present work, we aimed at studying how high PDT doses (LD_{95}s) administered in 1–3 cycles applied to HB4a-Ras cells,

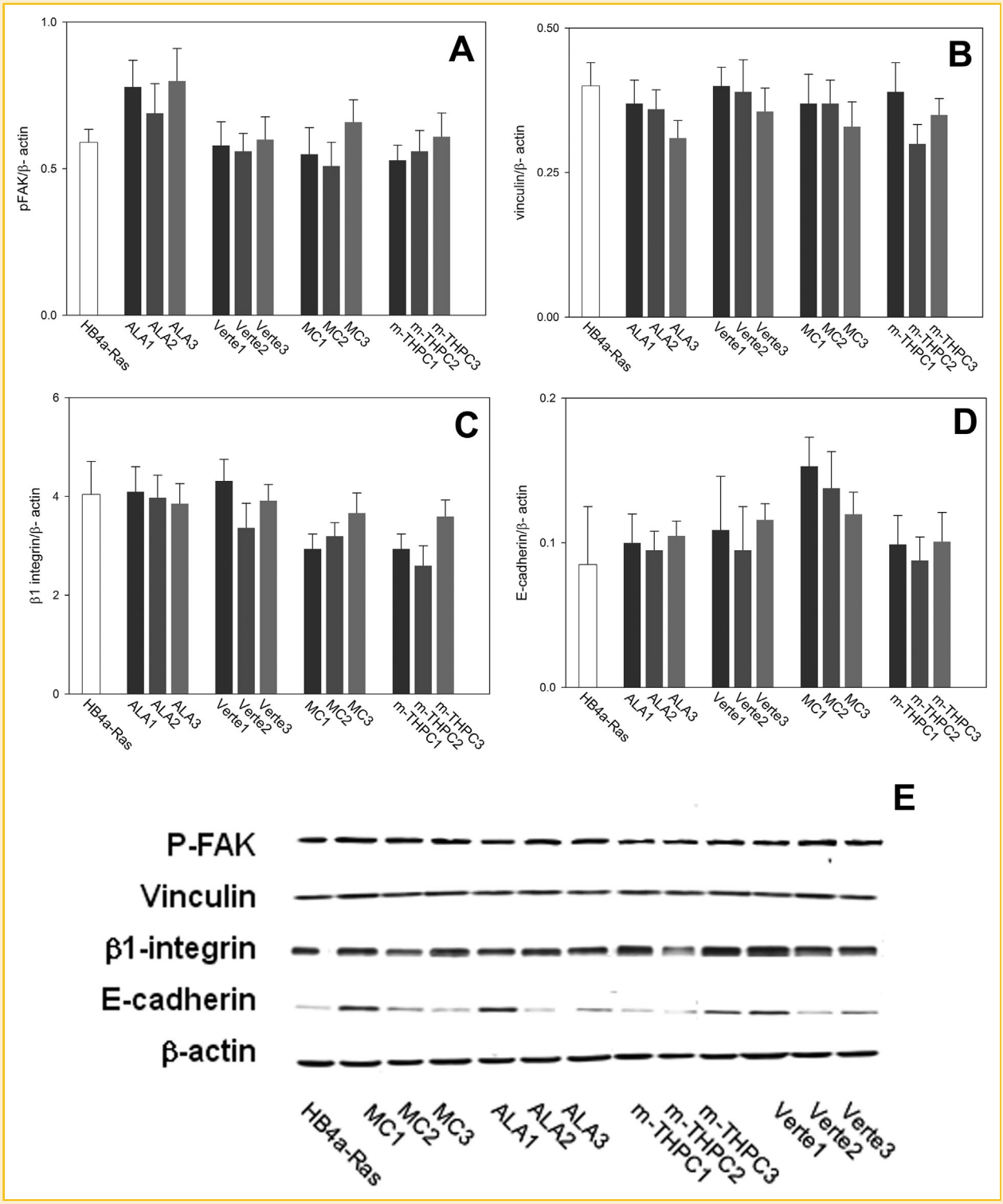

Fig. 7. Expression of p-FAK (A), vinculin (B), β1-integrin (C), and E-cadherin (D) on HB4a-Ras and PDT treated populations. Total extracts of subconfluent cultures were employed in Western blot assays. β-Actin was employed as a loading control. The figure E is representative of at least three independent experiments.

impacted on the invasive and migratory behavior in vitro, employing different PSs which act at different subcellular levels.

The modifications emerging after the successive PDT cycles may be either acquired in response to a selective pressure by the treatment or already expressed by a heterogeneous cell population and selected by the phototreatment [Casas et al., 2011].

Regardless of the PS used, the successive exposure to PDT cycles impacted negatively on the in vitro invasive and migratory

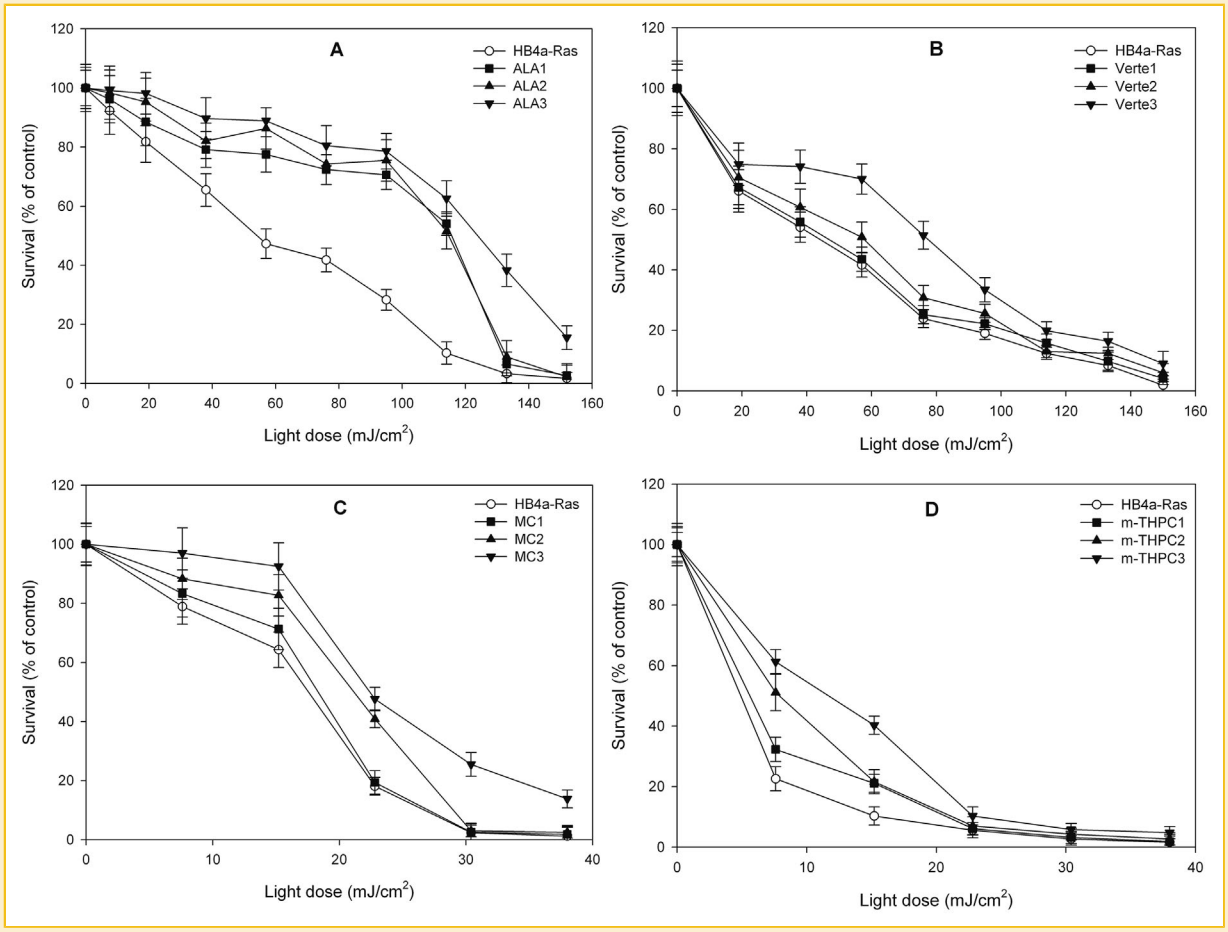

Fig. 8. Cell survival after PDT as a function of light dose concentration HB4a-Ras cells and its derived PDT-treated populations were incubated with of 1 mM ALA 3 h (A), 3 μg/ml MC 2 h (B), 2 μg/ml Verte 3 h (C), or 1 μg/ml m-THPC 3 h (D). Cells were irradiated with different light doses and cell survival was calculated after 19 h by the MTT assay. Points, average of four experiments performed in duplicate are shown. Bars represent means ± SD.

capacities, this impairment being proportional to the number of PDT cycles received.

HB4a-Ras transfected cells stained for F-actin revealed the presence of a circumferential actin rim and many cells presented short stress fibres mainly organized at the cell periphery and assembled in actin microspikes. These short stress fibres resembled the pattern of migrating cells, in which dorsal stress fibres are elongated primarily by the leading edge focal adhesions [Vallenius, 2013]. These features suggest that Ras induces the development of an invasive phenotype. Regardless of the PS employed, PDT-treated populations exhibited shorter stress fibres than the initial HB4a-Ras cells and the number of dorsal stress fibres appeared to be decreased in the PDT-treated populations. The circumferential actin filament remained present in most of the PDT-treated cells.

The cell morphology is strongly associated with alterations in the actin cytoskeleton [Pollard and Cooper, 2009]. One of the salient features of our PDT-treated populations was the increased loss of cell-to-cell interactions and the loss of epithelial shape. Changes in the morphology were already noticed in the ALA-PDT resistant clones isolated by us from the murine mammary adenocarcinoma LM3 [Casas et al., 2006], in which loss of epithelial features were also observed. In addition, and similarly to the mentioned resistant clones, our PDT surviving populations had decreased migratory and invasive capacities; although they presented a more undifferentiated shape than the parental line—a feature that is generally related to a more aggressive phenotype.

Actin has been identified as the main cytoskeleton component affected by PDT either at the early or at the late stages of photodamage. However, the changes induced in the structure of actin filaments seem to depend on the initial cell morphology [Di Venosa et al., 2015]. While some resistant cells show an F-actin disorganisation pattern [Casas et al., 2008a], in others, F-actin seems to be better organized in the resistant cells as compared to the parental ones. Besides, stress fibres are longer in the most PDT resistant populations [Milla et al., 2011]. It is noteworthy that PDT-treated populations are formed by a 5% of cells surviving the PDT process, and these surviving cells may be expressing a feature that is either selected or acquired during the process photosensitization. This phenomenon may explain the differences between resistant cells of different origins and obtaining procedures.

In addition, there is a strong relationship between the cortical actin and the catenin–cadherin complexes. Reversible actin

depolymerization affects the peripheral distribution of cadherin–catenin complexes [Quinlan and Hyatt, 1999]. Breast and other cancers that have upregulated Ras activity are often found to have downregulated or mislocalized E-cadherin expression [Li and Mattingly, 2008]. The loss of E-cadherin results in a loss of cell-to-cell adhesion together with the induction of multiple transcription factors, which favor the epithelial–mesenchymal transition and the consequent metastatic dissemination [Onder et al., 2008]. The phenomenon observed for E-cadherin in epithelial cells is not a static state; this process entails the constitutive internalization and trafficking back to the plasma membrane at the basolateral membrane, and is known to be under a fine cellular control [Angst et al., 2001]. Inhibition of Ras can restore E-cadherin expression in a variety of human cancer cells [Nam et al., 2002].

Alterations in the distribution but not in the expression of E-cadherin were observed in our LM3 mammary adenocarcinoma ALA-PDT resistant clones. These features were particularly marked in one of the two clones isolated, in which E-Cadherin was distributed as interdigitations, which account for a higher cell-to-cell cohesion and a higher differentiation level [Casas et al., 2008a]. However, other authors have not found similar changes of E-cadherin distribution in methyl-ALA PDT-resistant cells isolated from the SCC-13 squamous carcinoma cell line [Milla et al., 2011].

In terms of protein expression, subsequent PDT treatments did not induce clear modifications in E-Cadherin expression, although it is noteworthy that some of the populations displayed increased protein levels. However, the biological relevance is limited since the protein was mislocalized. And even when it is widely accepted that deregulation of E-cadherin adhesion is a crucial step during cell migration and metastasis [Hazan et al., 2004], taking into account the overall decreased migration and invasion capacities of our PDT-treated populations, it can be concluded that the E-cadherin expression changes driven by PDT cannot impact negatively on the metastatic capacity of the cells after photodamage.

We have also noticed that most of the PDT-treated populations were more adherent to plastic than HB4a-Ras cells. This increased adhesion correlated with the number of PDT cycles received, except for the Verte3 population, which resulted less adherent than the parental one. This feature, which was acquired during the successive PDT treatments, resembled the normal non-transfected HB4a cells.

Adhesion studies performed immediately after PDT often demonstrate a decreased adhesion either to ECM or to other cell types, but this pattern appears to be recovered at long periods of time after PDT [Di Venosa et al., 2015]. PDT-surviving cells do not show a consistent pattern of ECM cell adhesion modifications. On the other hand, adhesion to plastic and consequently, resistance to trypsinization seem to be factors usually affected after PDT, and cells surviving photodamage are usually more adherent to plastic [Casas et al., 2011].

Cell-to-ECM adhesion is regulated by specific cellular adhesion molecules known as integrins. The onset of drug resistance to chemotherapy phenotypes is often associated with altered expression of adhesion and cytoskeletal components [Thompson et al., 1992]. The adhesion changes can also determine the cellular shape. Due to the changes found in the cell adhesion and cell shape of the PDT-treated clones, in the present work we studied the expression of β1-integrin, vinculin, and *p*-FAK in HB4a-Ras and its derived PDT-treated subpopulations. However, we did not find a clear pattern of expression modification of these proteins involved in the cell adhesion processes. A certain degree of variation was found in the proteins expression of the different cells but these changes were ascribed to a random selection of the subpopulations.

Changes on integrin expression have been observed as a consequence of photodamage. However, the cell type is critical for the integrin response to PDT [Di Venosa et al., 2015]. The inhibition of cell adhesion to ECM proteins after Verte-PDT has been described. When the cell type exposed to PDT was OVCAR three ovarian carcinoma, the loss in adhesiveness was accompanied by a loss of β1 integrin-containing focal adhesion plaques [Runnels et al., 1999], whereas, the PDT performed on human foreskin fibroblasts did not induce any change in integrin expression, but it provoked a decrease in the FAK phosphorylation rate, this phenomenon being probably related to integrin signalling pathways [Margaron et al., 1997]. Our previously isolated ALA-PDT resistant LM3 mammary carcinoma clones exhibited higher binding to collagen I than the parental lines and without overexpressing β1 integrin [Casas et al., 2006].

The abnormal expression and polymerisation of actin are associated with the invasiveness and metastasis [Guo et al., 2013]. The onset of motility necessary for invasion requires a relaxation of static actin structures to form flexible membrane protrusions. Rigid actin stress fibres are disassembled upon the formation of dorsal ruffles, leaving a fine cortical actin meshwork behind, from which cell membrane protrusions like lamellipodia can emerge [Yilmaz and Christofori, 2009].

In the present study, the strong migratory capacity of HB4a-Ras cells was seen dramatically impaired in all the PDT-treated populations, thus resembling the parental HB4a normal cells. The migratory capacity was found to decrease with the number of PDT cycles for all the PSs employed. Even one PDT cycle was capable of significantly reducing the cell migration rate.

The reduced migration pattern resembled HB4a parental cells, which migrate twofold less than the *RAS* transfected ones.

Both MMP-9 and -2 activities were diminished in most of our PDT-treated populations, which might be quite relevant for invasion and metastasis. Expression of tumor matrix metalloproteinases has been shown to be either increased [Osiecka et al., 2010] or decreased by PDT treatment with several PSs [Etminan et al., 2011] either in tumors or in skin wound healing models.

A strong impact of PDT was also found in the in vitro invasion capacity of the HB4a-Ras cells. The capacity to invade Matrigel-coated transwells was decreased in all the populations and even completely impaired in the MC3 population, resembling again the features of HB4a cells which are not invasive.

The impairment of the cell invasion capacity seemed to be somewhat dependent on the type of PS employed. Even though mitochondria and lysosomes are also target organelles stained by MC [Chen et al., 2000], this dye also works as a membrane probe for the analysis of the metabolic states of both normal and cancer cells [Sieber et al., 1987]. It may be hypothesized that MC acting mainly at the cell membrane level is the PS which induced the most marked increases on adhesion to plastic, the less invasive phenotype and the most marked decrease on MMP activities.

Impaired migration and invasion capacities in vitro, together with a decreased activity of metalloproteinases observed in our PDT-treated populations suggest that the cells surviving PDT would be less metastatic than the initial population. These findings are in agreement with other authors [Di Venosa et al., 2015].

In vivo, evidences suggest that most cells surviving PDT have a decreased metastatic potential [Casas et al., 2009; Etminan et al., 2011]. On the other hand, Momma et al. [1998] have reported an increased impact on the metastatic capacity of PDT-surviving cells after sublethal PDT prostate cancer MatLyLu cells.

However, the metastatic capacity of in vitro PDT-treated cells when they are injected into mice could be quite different from the metastatic rate of an implanted tumor after in vivo PDT treatment. In this regard, the impact of PDT on the endothelial barrier becomes important [Di Venosa et al., 2015]. Xenograft assays in immunodeficient mice injected with Methyl-ALA-PDT-resistant squamous cell carcinomas revealed that the tumors generated by resistant cells were bigger than those induced by parental cells [Gilaberte et al., 2014].

In vitro, a decreased invasive and migratory phenotype of PDT-treated cells has been reported for a wide range of photosensitizers. Conversely, the migration of mesenchymal stem cells towards glioblastoma cells was enhanced after ALA-PDT treatment [Di Venosa et al., 2015]. However, we have found that ALA-PDT-adenocarcinoma resistant cells are less invasive and tend to migrate less in vitro. In vivo, these cells were found to induce less metastases foci as compared to the parental cell line. In addition, they showed a lower tumor take rate, latency time, and tumor growth rate and anchorage-dependent adhesion [Casas et al., 2008b].

To sum up, the key finding of this work is that mammary cells transfected with the *RAS* oncogene and surviving high doses of PDT exhibited decreased invasive and migratory capacities in vitro, resembling the non-tumoral, non-transfected HB4a cells. The findings presented herein encourage the use of PDT in combination with other treatments such as intraoperative procedures or post-surgery.

ACKNOWLEDGMENTS

This work was supported by the CONICET, the Science and Technology Argentine Agency PICT 2010-0772 and PICT 2008-0047. The authors are grateful to Prof Mike ÓHare for the provision of HB4a and HB4a-Ras cells and to Vanina Ripoll for her technical support.

REFERENCES

Angst BD, Marcozzi C, Magee AI. 2001. The cadherin superfamily: Diversity in form and function. J Cell Sci 114(Pt4):629–641.

Cai H, Wang Q, Luo J, Lim CK. 1999. Study of temoporfin metabolism by HPLC and electrospray mass spectrometry. Biomed Chromatogr 13:354–359.

Cai H, Wang YX, Zheng JC, Sun P, Yang ZY, Li YL, Liu XY, Li Q, Liu W. 2015. Photodynamic therapy in combination with CO_2 laser for the treatment of Bowen's disease. Lasers Med Sci 30(5):1505–1510.

Casas A, Battah S, Di Venosa G, Dobbin P, Rodriguez L, Fukuda H, Batlle A, MacRobert AJ. 2009. Sustained and efficient porphyrin generation in vivo using dendrimer conjugates of 5-ALA for photodynamic therapy. J Control Release 135(2):136–143.

Casas A, Fukuda H, Di Venosa G, Batlle A. 2001. Photosensitization and mechanism of cytotoxicity induced by the use of ALA derivatives in photodynamic therapy. Br J Cancer 85:279–284.

Casas A, Di Venosa G, Hasan T, Batlle A. 2011. Mechanisms of resistance to photodynamic therapy. Curr Med Chem 18(16):2486–2515.

Casas A, Di Venosa G, Vanzulli S, Perotti C, Mamome L, Rodriguez L, Simian M, Juarranz A, Pontiggia O, Hasan T, Batlle A. 2008b. Decreased metastatic phenotype in cells resistant to aminolevulinic acid-photodynamic therapy. Cancer Lett 271:342–351.

Casas A, Perotti C, Ortel B, Di Venosa G, Saccoliti M, Batlle A, Hasan T. 2006. Tumor cell lines resistant to ALA-mediated photodynamic therapy and possible tools to target surviving cells. Int J Oncol 29(2):397–405.

Casas A, Sanz-Rodriguez F, Di Venosa G, Rodriguez L, Mamone L, Blázquez A, Jaén P, Batlle A, Stockert JC, Juarranz A. 2008a. Disorganisation of cytoskeleton in cells resistant to photodynamic treatment with decreased metastatic phenotype. Cancer Lett 270(1):56–65.

Casas A, Di Venosa G, Batlle A, Fukuda H. 2002. In vitro photosensitisation of a murine mammary adenocarcinoma cell line with Verteporfin. Cell Mol Biol (Noisy-le-grand) 48(8):931–937.

Chen JY, Cheung NH, Fung MC, Wen JM, Leung WN, Mak NK. 2000. Subcellular localization of merocyanine 540 (MC540) and induction of apoptosis in murine myeloid leukemia cells. Photochem Photobiol 72(1):114–120.

Denizot L, Lang R. 1986. Rapid colorimetric assay for cell growth and survival modifications to the tetrazolium dye procedure giving improved sensitivity and reliability. J Immunol Methods 89:271–277.

Di Venosa G, Perotti C, Batlle A, Casas A. 2015. The role of cytoskeleton and adhesion proteins in the resistance to photodynamic therapy. Possible therapeutic interventions. Photochem Photobiol Sci 14(8):1 451–1464.

Di Venosa G, Rodriguez L, Mamone L, Gándara L, Rossetti MV, Batlle A, Casas A. 2012. Changes in actin and E-cadherin expression induced by 5-aminolevulinic acid photodynamic therapy in normal and Ras-transfected human mammary cell lines. J Photochem Photobiol B 106:47–52.

Diwu Z, Lown JW. 1994. Phototherapeutic potential of alternative photosensitizers to porphyrins. Pharmacol Ther 63(1):1–35.

Dougherty TJ. 2002. An update on photodynamic therapy applications. J Clin Laser Med Surg 20(1):3–7.

Dolmans DE, Fukumura D, Jain RK. 2003. Photodynamic therapy for cancer. Nat Rev Cancer 3(5):380–387.

Etminan N, Peters C, Ficnar J, Anlasik S, Bünemann E, Slotty PJ, Hänggi D, Steiger HJ, Sorg RV, Stummer W. 2011. Modulation of migratory activity and invasiveness of human glioma spheroids following 5-aminolevulinic acid-based photodynamic treatment. Laboratory investigation. J Neurosurg 115(2):281–288.

Gilaberte Y, Milla L, Salazar N, Vera-Alvarez J, Kourani O, Damian A, Rivarola V, Roca MJ, Espada J, González S, Juarranz A. 2014. Cellular intrinsic factors involved in the resistance of squamous cell carcinoma to photodynamic therapy. J Invest Dermatol 134(9):2428–2437.

Guo C, Liu S, Wang J, Sun MZ, Greenaway FT. 2013. ACTB in cancer. Clin Chim Acta 417:39–44.

Hazan RB, Qiao R, Keren R, Badano I, Suyama K. 2004. Cadherin switch in tumor progression. Ann NY Acad Sci 1014:155–163.

Kelty C, Brown N, Reed M, Ackroyd R. 2002. The use of 5-aminolaevulinic acid as a photosensitiser in photodynamic therapy and photodiagnosis. Photochem Photobiol Sci 1:158–168.

Lambrechts A, Troys M, Ampe C. 2004. The actin cytoskeleton in normal and pathological cell motility. Int J Biochem Cell Biol 36:1890–1909.

Leung WN, Sun X, Mak NK, Yow CM. 2002. Photodynamic effects of mTHPC on human colon adenocarcinoma cells: Photocytotoxicity, subcellular localization and apoptosis. Photochem Photobiol 75(4):406–411.

Li Q, Mattingly RR. 2008. Restoration of E-cadherin cell-cell junctions requires both expression of E-cadherin and suppression of ERK MAP kinase activation in Ras-transformed breast epithelial cells. Neoplasia 10(12):1444–1458.

Li T, Guo H, Song Y, Zhao X, Shi Y, Lu Y, Hu S, Nie Y, Fan D, Wu K. 2014. Loss of vinculin and membrane-bound β-catenin promotes metastasis and predicts poor prognosis in colorectal cancer. Mol Cancer 13:263.

Margaron P, Sorrenti R, Levy JG. 1997. Photodynamic therapy inhibits cell adhesion without altering integrin expression. Biochim Biophys Acta 1359:200–210.

Meier D, Campanile C, Botter SM, Born W, Fuchs B. 2014. Cytotoxic efficacy of photodynamic therapy in osteosarcoma cells in vitro. J Vis Exp 85:51213.

Milla LN, Cogno IS, Rodríguez ME, Sanz-Rodríguez F, Zamarrón A, Gilaberte Y, Carrasco E, Rivarola VA, Juarranz A. 2011. Isolation and characterization of squamous carcinoma cells resistant to photodynamic therapy. J Cell Biochem 112(9):2266–2278.

Momma T, Hamblin M, Wu H, Hasan T. 1998. Photodynamic therapy of orthotopic prostate cancer with benzoderivative: Local control and distant metastasis. Cancer Res 58:5425–5431.

Nam JS, Ino Y, Sakamoto M, Hirohashi S. 2002. Ras farnesylation inhibitor FTI-277 restores the E-cadherin/catenin cell adhesion system in human cancer cells and reduces cancer metastasis. Jpn J Cancer Res 93:1020–1028.

Onder TT, Gupta PB, Mani SA, Yang J, Lander ES, Weinberg RA. 2008. Loss of E-cadherin promotes metastasis via multiple downstream transcriptional pathways. Cancer Res 68(10):3645–3654.

Osiecka B, Jurczyszyn K, Symonowicz K, Bronowicz A, Ostasiewicz P, Czapińska E, Hotowy K, Krzystek-Korpacka M, Gebarowska E, Izykowska I, Dziegiel P, Terlecki G, Ziółkowski P. 2010. In vitro and in vivo matrix metalloproteinase expression after photodynamic therapy with a liposomal formulation of aminolevulinic acid and its methyl ester. Cell Mol Biol Lett 15(4):630–650.

Pellegrin S, Mellor H. 2007. Actin stress fibres. J Cell Sci 120(Pt20):3491–3499.

Pollard TD, Cooper JA. 2009. Actin, a central player in cell shape and movement. Science 326(5957):1208–1212.

Quinlan MP, Hyatt JL. 1999. Establishment of the circumferential actin filament network is a prerequisite for localization of the cadherin-catenin complex in epithelial cells. Cell Growth Differ 10(12):839–854.

Rodriguez L, Di Venosa G, Batlle A, Macrobert A, Casas A. 2007. Response to ALA based PDT in an immortalised normal breast cell line and its counterpart transformed with the Ras oncogene. Photochem Photobiol Sci 6(12): 1306–1310.

Rodriguez-Viciana P, Tetsu O, Oda K, Okada J, Rauen K, McCormick F. 2005. Cancer targets in the Ras pathway. Cold Spring Harb Symp Quant Biol 70:461–467.

Rundquist I, Olsson M, Brunk U. 1984. Cytofluorometric quantitation of acridine orange uptake by cultured cells. Acta Pathol Microbiol Immunol Scand A 92:303–309.

Runnels JM, Chen N, Ortel B, Kato D, Hasan T. 1999. BPD-MA mediated photosensitization in vitro and in vivo: Cellular adhesion and beta1 integrin expression in ovarian cancer cells. Br J Cancer 80:946–953.

Rusnak D, Affleck K, Cockerill S, Stubberfield C, Harris R, Page M. 2001. The characterization of novel, dual erbB-2/EGFR, tyrosine kinase inhibitors: Potential therapy for cancer. Cancer Res 61:7196–7203.

Sieber F, O'Brien JM, Krueger GJ, Schober SL, Burns WH, Sharkis SJ, Sensenbrenner LL. 1987. Antiviral activity of merocyanine 540. Photochem Photobiol 46:707–711.

Stamps A, Davies SC, Burman J, O'Hare MJ. 1994. Analysis of proviral integration in human mammary epithelial cell lines immortalized by retroviral infection with a temperature-sensitive SV40 T-antigen construct. Int J Cancer 57:1–10.

Stockert JC, Juarranz A, Villanueva A, Nonell S, Horobin RW, Soltermann AT, Durantini EN, Rivarola V, Colombo LL, Espada J, Cañete M. 2004. Photodynamic therapy: Selective uptake of photosensitizing drugs into tumor cells. Cur Topics Pharmacol 8:185–217.

Sulzmaier FJ, Jean C, Schlaepfer DD. 2014. FAK in cancer: Mechanistic findings and clinical applications. Nat Rev Cancer 14(9):598–610.

Tanghetti EA, Hamann C, Tanghetti M. 2015. A controlled comparison study of topical fluourouracil 5% cream pre-treatment of aminolevulinic Acid/ Photodynamic therapy for actinic keratosis. J Drugs Dermatol 14(11): 1241–1244.

Thompson E, Paik S, Brunner N, Sommers C, Zugmaier G, Clarke R, Shima T, Torri J, Donhaue S, Lippman M, Martin G, Dickson R. 1992. Association of increased basement membrane invasiveness with absence of estrogen receptor and expression of vimentin in human breast cancer cell lines. J Cell Physiol 150:534–544.

Vallenius T. 2013. Actin stress fibre subtypes in mesenchymal migrating cells. Open Biol 3(6):130001.

Yilmaz M, Christofori G. 2009. EMT, the cytoskeleton, and cancer cell invasion. Cancer Metastasis Rev 28(1–2):15–33.